Electric field control of electromagnon frequency in multiferroics

S. Omid Sayedaghaee,[1] Charles Paillard,[2] Sergey Prosandeev,[1] Sergei Prokhorenko,[1] Yousra Nahas,[1] Bin Xu,[3] and L. Bellaiche[1]

[1]*Physics Department and Institute for Nanoscience and Engineering, University of Arkansas, Fayetteville, Arkansas 72701, USA*
[2]*Université Paris-Saclay, CentraleSupélec, CNRS, Laboratoire SPMS, 91190 Gif-sur-Yvette, France*
[3]*Institute of Theoretical and Applied Physics, Jiangsu Key Laboratory of Thin Films, School of Physical Science and Technology, Soochow University, Suzhou 215006, China*

(Received 14 August 2022; accepted 1 November 2022; published 6 December 2022)

Electromagnons, which are coupled polar and magnetic excitations in magnetoelectric materials, are of large interest for electronic and computing technological devices. Using molecular dynamics simulations based on an *ab initio* effective Hamiltonian, we predict that the frequency of several electromagnons can be tuned by the application of electric fields in the model multiferroic $BiFeO_3$, with this frequency either increasing or decreasing depending on the selected electromagnon. In particular, we show that the frequency of electromagnons localized at ferroelectric domain walls can be tuned over a 200 GHz range by realistic dc electric fields. We interpret the realized frequency increase (decrease) by local hardening (softening) of the associated polar phonons which couples to the applied electric field. The increase versus decrease in the electromagnon frequency is further found to be correlated with the real-space localization of such phonons.

DOI: 10.1103/PhysRevMaterials.6.124404

I. INTRODUCTION

Electromagnons, a coupled oscillation wave of electrical and magnetic dipoles in magnetoelectric materials, have bolstered large interest since they were first discussed in the 1970s [1,2]. They have remained elusive for a long time, except in a few materials such as rare-earth (R) manganites $RMnO_3$ [3–5] and RMn_2O_5 [6,7] and ferrite perovskite oxides [8–11]. Among them, $BiFeO_3$ (BFO), a room temperature multiferroic [12], has been one of the most intensely considered magnetoelectrics for electromagnon detection, characterization, and technological applications. Among the various experimental and theoretical studies of electromagnons, most have focused on so-called electroactive magnons, i.e., control of spin waves by electric fields [13–17]. On the other hand, much less work has been devoted to the study of magnetic control of polarization waves, with a few theoretical works realized in $BiFeO_3$ [18–20] and manganites [21]. The present work goes one step further by bridging the two approaches, as we intend to demonstrate the possibility of resonantly exciting electromagnons (induced by ferroelectric domain walls) using ac magnetic fields while concurrently manipulating their frequency with dc electric fields.

Note that ferroelectric domain walls can now routinely be written, erased, and reconfigured using, for instance, piezoforce microscopy [22–25]. The ability to generate magnetically polarization waves localized at domain walls, as proposed in Ref. [20], already promises the tantalizing possibility of reconfigurable nanometer-size electrical circuits, whose power is switched on and sustained remotely by ac magnetic fields. If now one is able to act on the electrical polarized waves localized at the ferroelectric domain walls, for instance, using local electric fields, one could dream of achieving reconfigurable logical elements for computing or detection.

In this paper, we investigate how dc electric fields affect the domain-wall-induced electromagnons evidenced in Ref. [20] in multiferroic $BiFeO_3$. Using molecular dynamics based on an *ab initio* effective Hamiltonian, we reveal that the frequency of these electromagnons is rather sensitive to these dc fields, either increasing or decreasing with them depending on the chosen electromagnon. This latter different behavior (namely, increase versus decrease) is found to be correlated with the real-space localization of the optical phonon associated with these electromagnons.

II. METHODS

Here and as shown in Fig. 1, we simulate a multidomain system of BFO with 180° domain configuration inside which two types of domains alternate along the [110] pseudocubic direction. The first type of domain, denoted as domain D1, is shown in red in Fig. 1 and possesses electric dipoles aligned along the $[\bar{1}11]$ direction. The second kind of domain, coined domain D2, is displayed in blue in this figure and exhibits electric dipoles lying along the opposite $[1\bar{1}\bar{1}]$ direction. In both domains the magnetic moments and antiferromagnetic (AFM) moments are along the perpendicular [211] and $[0\bar{1}1]$ directions, respectively.

The energetics and properties of the studied system are modeled via use of the effective Hamiltonian framework detailed in Ref. [26] within a molecular dynamics (MD) approach [27], in order to obtain dynamical properties. Technically, Newtonian equations of motion are used to investigate

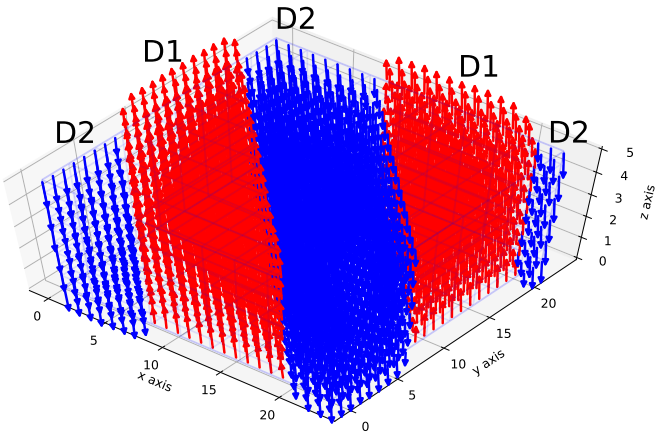

FIG. 1. Schematic representation of the zero-field electric dipole moments' pattern for our studied $24 \times 24 \times 6$ supercell of $BiFeO_3$. The blue and red vectors are used to represent electric dipole moments along the $[1\bar{1}\bar{1}]$ and $[\bar{1}11]$ directions, respectively.

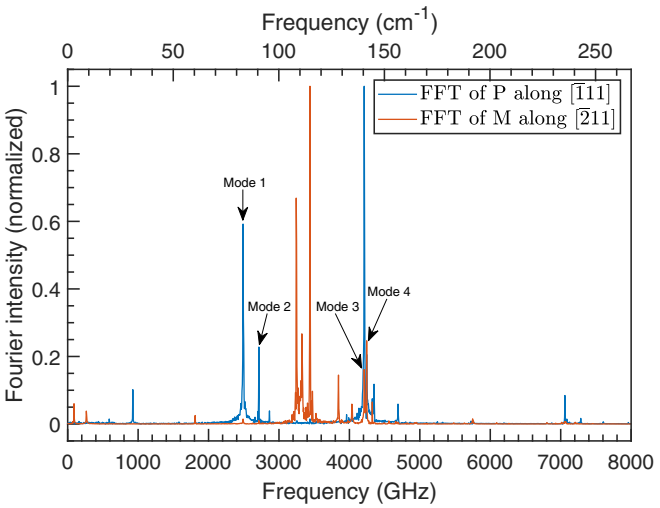

FIG. 2. Fourier analyses of polarization (P) and magnetization (M). The frequency spectrum of the component of electrical dipole moments along the $[\bar{1}11]$ direction (blue) and magnetic moments along the [211] direction (orange) obtained by Fourier analysis when the applied dc electric field is 1×10^7 V/m. The frequency of the modes shown by black arrows significantly shifts upon applying different magnitudes of electric field.

the dynamics of the ionic degrees of freedom of this effective Hamiltonian: These dynamics are local modes which are directly proportional to local electric dipoles inside each five-atom cell, pseudovectors representing the antiferrodistortive motions inside such five-atom cells, and both homogeneous and inhomogeneous strain components. Regarding the dynamics of the magnetic moments, the approach of Ref. [28] is followed, for which such dynamics are treated through the Landau-Lifshitz-Gilbert (LLG) equation [29].

We applied dc electric fields with magnitude ranging between 1.0×10^7 and 1.0×10^8 V/m along the $[\bar{1}11]$ direction to such a multidomain, which is currently mimicked by using a $24 \times 24 \times 6$ supercell. It should be noted that an electric field of magnitude 2.0×10^8 V/m is strong enough to reorient all dipole moments along its direction and convert the configuration to a monodomain. The MD simulations are conducted at a temperature of 10 K. To ensure that the magnetic moments only slightly fluctuate about the same direction during the course of simulations, a dc magnetic field of magnitude 245 T is applied along the [211] direction. A lower magnetic field (which is accessible in practical applications) could be applied. In fact, we also performed simulations with a dc magnetic field having a magnitude of 2.45 T along the [211] direction, and we obtained similar results. Such a large magnetic field and low temperature were chosen here to avoid large fluctuations of magnetic properties and see the results more clearly. Each MD simulation was performed for 1 000 000 steps of 0.5 fs each, while both homogeneous and inhomogeneous strains were relaxed.

III. RESULTS AND DISCUSSION

It is important to realize that, under zero dc electric field, there is no macroscopic polarization, as a result of the cancellations between the polarizations of domains D1 and D2. On the other hand, we numerically found that the application of our considered dc electric fields results in an increase in the magnitude of electric dipoles in the domain D1 regions and its reduction in the domain D2 areas, therefore yielding now a finite overall polarization along the direction of the applied field, which is $[\bar{1}11]$. It is worth mentioning that we observed the change in the structure from a 180° multidomain to a monodomain when the applied electric field exceeds a threshold ($E_{\text{thresh}} = 2 \times 10^8$ V/m) which is rather abrupt—at least with the resolution of the applied electric field change here, being $E = 1 \times 10^7$ V/m. One may thus need a much smaller step in the field's magnitude to observe motion of the domain walls. One can also increase the temperature to see such motion. For instance, and as shown in the Supplemental Material [30], motion of the domain walls does occur at $T = 300$ K when the applied electric field varies from $E = 3 \times 10^7$ to $E = 5 \times 10^7$ V/m.

We then perform Fourier analysis of the temporal evolution of this resulting electrical polarization along the $[\bar{1}11]$ direction, and that of the magnetization along the [211] direction. Figure 2 shows the resulting fast Fourier transformations (FFTs) of both the electrical polarization and magnetization for a dc electric field of 1.0×10^7 V/m, which reveals the existence of frequency modes presenting phonons and magnons. Here, in particular, some peaks are observed at the same frequency in the FFT spectrum of both polarization and magnetization, which is a signature of electromagnons. Within the electromagnonic modes that are observed here, four modes are of particular interest due to their noticeable frequency shift as a response to the application of electric fields of various magnitudes. These modes are denoted as modes 1, 2, 3, and 4 in Fig. 2 (note that these four modes have very similar frequencies to those one can guess to be around 90 cm^{-1} ($\simeq$2700 GHz) and 140 cm^{-1} ($\simeq$4200 GHz) in the Supplemental Material of Ref. [31] for precisely 180° domains of BFO). The electric-field-induced frequency shift of both the phonon

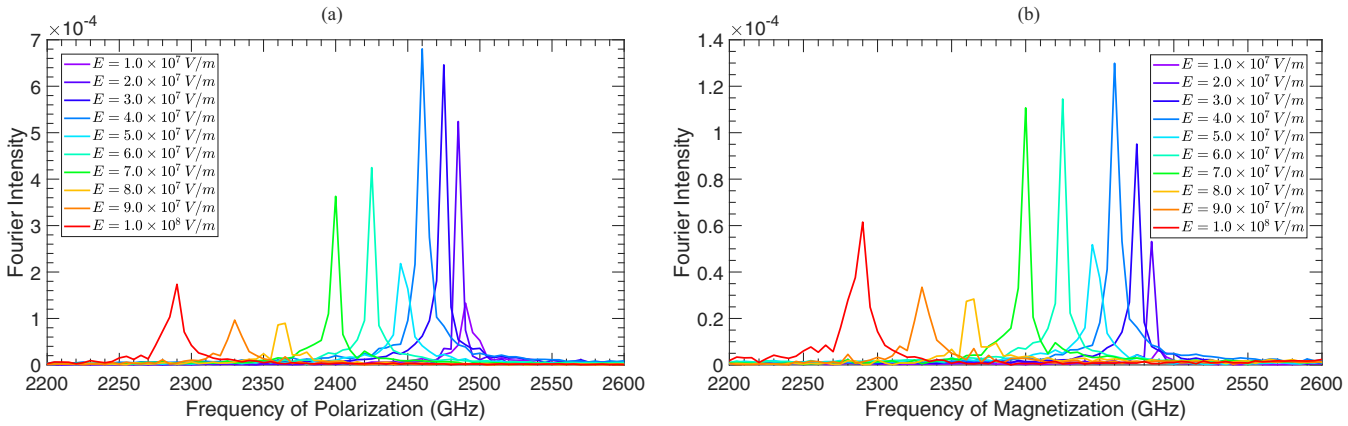

FIG. 3. Frequency shift of optical phonons and magnons of mode 1. (a) The shift of the frequency observed for the optical phonons upon the application of various dc electric fields. (b) The shift of the frequency observed for the magnons upon the application of various dc electric fields. For both cases the applied electric field changes from 1.0×10^7 to 1.0×10^8 V/m.

and magnon associated with the electromagnonic mode 1 is demonstrated in Figs. 3(a) and 3(b), respectively. For this mode, as indicated by purple solid lines in Figs. 3(a) and 3(b), when the applied electric field is 1.0×10^7 V/m the phonon peak is at 2490 GHz [Fig. 3(a)] and the magnon peak is at exactly the same frequency location [Fig. 3(b)]. When the applied electric field increases to higher magnitudes, the frequency of the phonon and magnon decrease concurrently, which results in a softening for mode 1. It should be noted that, in multiferroics, strain can contribute to the emergence of so-called electroacoustic magnons as a mixture of acoustic phonons, optical phonons, and magnons [18,19]. Here, we numerically found (not shown here) that the four aforementioned modes are present in the frequency spectrum of both the polarization and magnetization even if the homogeneous strain is clamped during the course of MD simulations, which clarifies that these modes are electromagnons consisting of optical phonons and magnons. It should be noted that we do not believe that these computed intensities of Fig. 3 have a real physical meaning in our simulations, since such intensities are not monotonic with the fields and can vary when slightly changing some technical details of the Fourier transform (especially considering the small values of the vertical scale in the figure). On the other hand, the frequency position of these peaks is insensitive to such details and does carry physical significance.

For each of these four considered modes, the evolution of their frequency as a function of the magnitude of the dc electric field is shown in Fig. 4. One can see that mode 1 experiences a rather strong decrease in its frequency when the electric field varies from 1.0×10^7 to 1.0×10^8 V/m, namely, by about 200 GHz from 2490 to 2290 GHz. Note that it is known that the effective Hamiltonians of BFO overestimate the magnitude of electric fields by a factor of 23 [32]. Hence our maximum applied electric field would correspond experimentally to approximately 43 kV/cm, which is easily sustained in $BiFeO_3$ thin films [33]. Note also that the decrease in the mode 1 frequency appears to be quadratic in nature. Mode 2 also adopts a reduction of its frequency, but to a smaller extent (that is, by about 55 GHz from 2715 to 2660 GHz) and in a linear fashion, with a rate of 0.06 GHz/(kV/cm). Interestingly, such linear variation has indeed been observed in $BiFeO_3$ for some electromagnons. For instance, the frequency of the so-called extracyclon mode ψ_2 may increase or decrease (depending on whether the electric field increases or decreases the polarization) with a rate of approximately 1.3 GHz/(kV/cm) [34]. In the same reference, the cyclon mode ϕ_2 shows an opposite behavior with the rate of ≈0.24 GHz/(kV/cm). Note that we focus here on domain-wall-induced electromagnons with an antiferromagnetic structure, while the cyclon and extracyclon modes considered in Ref. [34] are modes in a monodomain single crystal having a magnetic cycloidal state. In addition, the commonly known overestimation of electric fields in effective Hamiltonian models may also contribute to the difference between computational and experimental rates for the dc-field-induced change in frequency. As a matter of fact, rescaling our theoretical fields by dividing them by 23 (as indicated in Ref. [32]) results in a rate for our mode 2 that goes from 0.06 to 1.38 GHz/(kV/cm), which is similar to the observed magnitude of such rate for the ψ_2 mode in Ref. [34]. Similarly, mode 3 has the same kind of qualitative behavior as mode 2 but with about twice the slope—that is, a linear decrease in its frequency by ≃117 GHz when the dc electric field strengthens from 1.0×10^7 to 1.0×10^8 V/m. Strikingly, mode 4, whose frequency is basically that of mode 3 for an interpolated zero field, adopts a mirror behavior with respect to mode 3, in the sense that its frequency concomitantly increases by a similar amount of ≃117 GHz in a linear fashion. Note that we also performed simulations with *opposite* dc electric fields (i.e., along $[1\bar{1}\bar{1}]$), which allows us to further determine that the frequencies of modes 1 and 2 depend on the *magnitude* of the electric field along $[\bar{1}11]$ or $[1\bar{1}\bar{1}]$ while those of modes 3 and 4 linearly depend on the *projection* of the electric field along $[\bar{1}11]$ (i.e., not only on the magnitude but also on the sign of this projection).

In order to understand all these behaviors and demonstrate their relationship with real-space localization, a layer-by-layer analysis is performed at the different planes that are parallel to the domain wall. More precisely, the Fourier transform of the average of polarization of each of these planes is computed for the frequencies associated with the four aforementioned

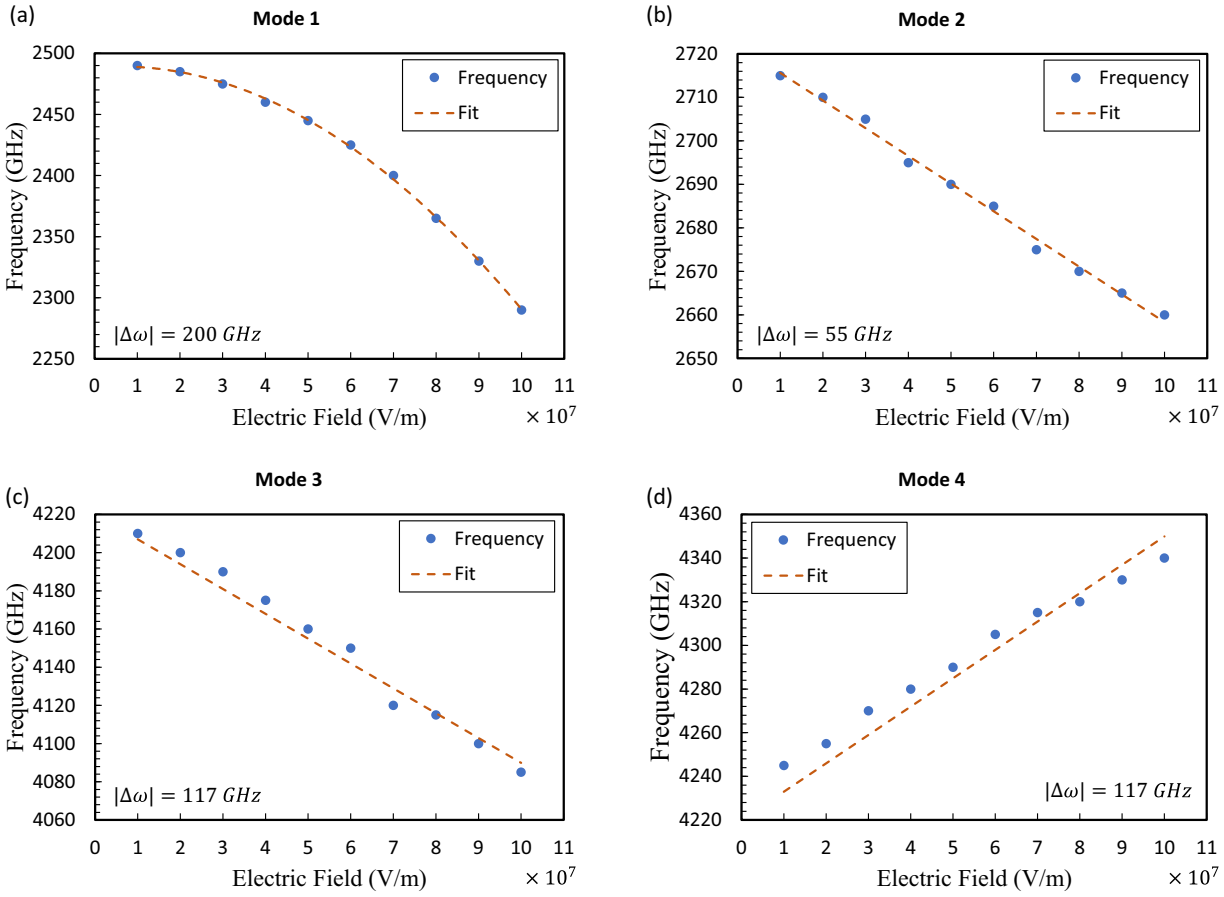

FIG. 4. (a)–(d) Frequency shift of four electromagnons. In each panel, the frequency shift of the corresponding mode vs the applied electric fields is shown. A polynomial fit of second order for mode 1 and of first order for modes 2, 3, and 4 is applied. $|\Delta\omega|$ is the magnitude of the difference between the highest and the lowest frequencies of the fitted lines for our chosen range of applied electric fields.

modes for a dc field of 1.0×10^7 V/m and is shown in Fig. 5. For instance, Fig. 5(a) tells us that mode 1 is a mode that is strongly localized at the domain walls. Furthermore, Fig. 5(b) reveals that mode 2 also localizes near the domain walls but to a smaller extent, as seen by comparing its vertical scale with that of Fig. 5(a). Consequently, by looking at Figs. 4(a), 4(b), 5(a), and 5(b), one can conclude that modes localizing near the domain walls soften under a dc electric field, that is, they have their frequency decreasing when the field increases—and such decrease is larger when the localization near the walls is stronger.

Interestingly, Figs. 5(c) and 5(d) tell us that modes 3 and 4 are rather different from modes 1 and 2, in the sense that they prefer to localize inside the domains rather than at the domain walls. More precisely, mode 3 reaches its maximum of the Fourier transform of the polarization in the domain D2 region inside which the polarization is antiparallel to the applied electric field. Consequently, applying such a field will decrease the magnitude of the polarization in the domain D2 area, which corresponds to a local softening of the optical phonon, hence explaining the decrease in the frequency seen in Fig. 4(c) for mode 3. In contrast, mode 4 preferentially localizes in the domain D1 area for which the polarization is parallel to the dc electric field, and, as a result, such polarization increases in magnitude when the field strengthens. Such increase leads to a local hardening of mode 4 and therefore to a frequency that now increases with the field. Note that modes 3 and 4 (whose frequencies are about 4210 and 4245 GHz for a field of 1.0×10^7 V/m, which correspond to 140 and 142 cm^{-1}, respectively) can be thought of as both originating from the known zone-center optical phonon of the $BiFeO_3$ monodomain, which then splits in two under dc electric fields because of the existence of domain walls and two different types of domains in our studied system. Based on previous works on $BiFeO_3$ monodomain single crystals and the fact that we numerically further found (not shown here) that modes 3 and 4 have rather small FFTs of the component of the polarization along the [110] direction (which is perpendicular to the polarizations of both domain D1 and domain D2), one can suggest that modes 3 and 4 originate from the A_1 longitudinal optical (LO) mode, rather than the E transverse optical (TO) mode, of the $BiFeO_3$ monodomain [28,35–38].

IV. SUMMARY

In summary, we used an atomistic effective Hamiltonian to reveal that the frequency of electromagnons can be significantly tuned by applying dc electric fields in the prototypical

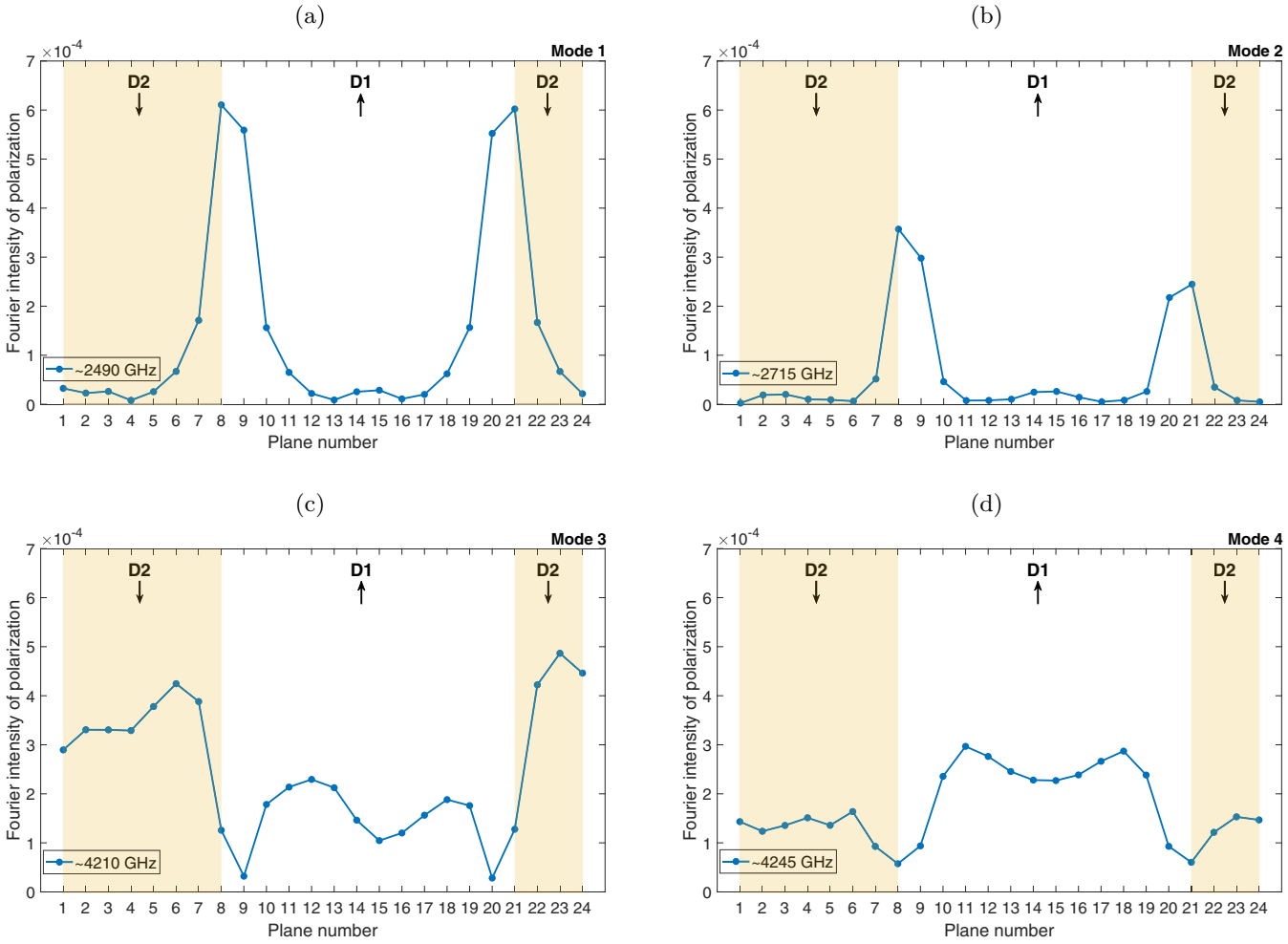

FIG. 5. (a)–(d) The degree of localization of the electromagnons possessing significant frequency shift under the application of electric fields. In each panel, the degree of localization of the corresponding mode at the planes parallel to the domain walls within the investigated supercell is shown. The shaded area corresponds to the domains possessing electric dipoles pointing along the $[1\bar{1}\bar{1}]$ direction, while the white area corresponds to the domains possessing electric dipoles pointing along the opposite $[\bar{1}11]$ direction. The arrow in each domain indicates the direction of the z component of electric dipole moments present in the domain. The applied electric field for all cases is $E = 1.0 \times 10^7$ V/m along the $[\bar{1}11]$ direction, which is parallel to the direction of the electric dipoles in domain D1 and antiparallel to the direction of the electric dipoles in domain D2.

$BiFeO_3$ multiferroic adopting ferroelectric domains. Such a finding is promising in terms of the design of novel devices taking advantage of the dual electric and magnetic nature of electromagnons, with the additional conveniences demonstrated here that (1) it should thus be possible to select the desired operating frequency by choosing the right combination of ac magnetic field frequency and magnitude of the dc electric field (in order to activate such electromagnons at this desired frequency) and (2) some of these electromagnons are localized at the ferroelectric domain walls, therefore rendering feasible application of local electric fields for realizing reconfigurable logical elements for computing or detection. These domain-wall-induced electromagnons are further found to either increase or decrease their frequencies under the dc electric fields, depending on the real-space localization of their associated phonons—that is, at the ferroelectric domain walls or at the "up" versus "down" domains. We therefore hope that the present study deepens the fascinating fields of electromagnons, ferroelectric domains, and magnonics.

ACKNOWLEDGMENTS

The authors acknowledge Vannevar Bush Faculty Fellowship (VBFF) Grant No. N00014-20-1-2834 from the Department of Defense and ARO Grant No. W911NF-21-1-0113. C.P. acknowledges ANR Grant No. ANR-21-CE24-0032 "Superspin" and a public grant overseen by the ANR as part of the Investissements d'Avenir program (Reference No. ANR-10-LABX-0035, Labex-NanoSaclay). S. Prosandeev also acknowledges ONR Grant No. N00014-21-1-2086. B.X. further acknowledges the financial support from National Natural Science Foundation of China under Grant No. 12074277, the startup fund from Soochow University, and the support from Priority Academic Program Development (PAPD) of Jiangsu Higher Education Institutions. S. Prokhorenko and Y.N. acknowledge ARO Grant No. W911NF-21-2-0162 (ETHOS). The authors also acknowledge the High Performance Computing Center at the University of Arkansas and thank Jorge Íñiguez for useful discussions.

[1] V. Baryakhtar and I. Chupis, Sov. Phys. Solid State **11**, 2628 (1970).

[2] G. A. Smolenski and I. E. Chupis, Sov. Phys.-Usp. **25**, 475 (1982).

[3] A. Pimenov, A. A. Mukhin, V. Y. Ivanov, V. D. Travkin, A. M. Balbashov, and A. Loidl, Nat. Phys. **2**, 97 (2006).

[4] A. Pimenov, T. Rudolf, F. Mayr, A. Loidl, A. A. Mukhin, and A. M. Balbashov, Phys. Rev. B **74**, 100403(R) (2006).

[5] P. Rovillain, M. Cazayous, Y. Gallais, M.-A. Measson, A. Sacuto, H. Sakata, and M. Mochizuki, Phys. Rev. Lett. **107**, 027202 (2011).

[6] A. B. Sushkov, R. V. Aguilar, S. Park, S.-W. Cheong, and H. D. Drew, Phys. Rev. Lett. **98**, 027202 (2007).

[7] A. B. Sushkov, M. Mostovoy, R. Valdés Aguilar, S.-W. Cheong, and H. D. Drew, J. Phys.: Condens. Matter **20**, 434210 (2008).

[8] T. N. Stanislavchuk, Y. Wang, Y. Janssen, G. L. Carr, S.-W. Cheong, and A. A. Sirenko, Phys. Rev. B **93**, 094403 (2016).

[9] M. Cazayous, Y. Gallais, A. Sacuto, R. de Sousa, D. Lebeugle, and D. Colson, Phys. Rev. Lett. **101**, 037601 (2008).

[10] P. Rovillain, M. Cazayous, Y. Gallais, A. Sacuto, R. P. S. M. Lobo, D. Lebeugle, and D. Colson, Phys. Rev. B **79**, 180411(R) (2009).

[11] S. Skiadopoulou, V. Goian, C. Kadlec, F. Kadlec, X. F. Bai, I. C. Infante, B. Dkhil, C. Adamo, D. G. Schlom, and S. Kamba, Phys. Rev. B **91**, 174108 (2015).

[12] D. Lebeugle, D. Colson, A. Forget, M. Viret, P. Bonville, J. F. Marucco, and S. Fusil, Phys. Rev. B **76**, 024116 (2007).

[13] R. de Sousa and J. E. Moore, Appl. Phys. Lett. **92**, 022514 (2008).

[14] C.-M. Chang, B. K. Mani, S. Lisenkov, and I. Ponomareva, Ferroelectrics **494**, 68 (2016).

[15] S. Seki, N. Kida, S. Kumakura, R. Shimano, and Y. Tokura, Phys. Rev. Lett. **105**, 097207 (2010).

[16] H. B. Chen, Y. Q. Li, and J. Berakdar, J. Appl. Phys. **117**, 043910 (2015).

[17] M. D. Davydova, K. A. Zvezdin, A. A. Mukhin, and A. K. Zvezdin, Phys. Sci. Rev. **5**, 20190070 (2020).

[18] S. O. Sayedaghaee, B. Xu, S. Prosandeev, C. Paillard, and L. Bellaiche, Phys. Rev. Lett. **122**, 097601 (2019).

[19] S. O. Sayedaghaee, C. Paillard, S. Prosandeev, B. Xu, and L. Bellaiche, npj Comput. Mater. **6**, 60 (2020).

[20] S. O. Sayedaghaee, S. Prosandeev, S. Prokhorenko, Y. Nahas, C. Paillard, B. Xu, and L. Bellaiche, Phys. Rev. Mater. **6**, 034403 (2022).

[21] M. P. V. Stenberg and R. de Sousa, Phys. Rev. B **80**, 094419 (2009).

[22] M. Lachheb, Q. Zhu, S. Fusil, Q. Wu, C. Carrétéro, A. Vecchiola, M. Bibes, D. Martinotti, C. Mathieu, C. Lubin, A. Pancotti, X. Li-Bourrelier, A. Gloter, B. Dkhil, V. Garcia, and N. Barrett, Phys. Rev. Mater. **5**, 024410 (2021).

[23] S. Cherifi, R. Hertel, S. Fusil, H. Béa, K. Bouzehouane, J. Allibe, M. Bibes, and A. Barthélémy, Phys. Status Solidi RRL **4**, 22 (2010).

[24] A. Gruverman, M. Alexe, and D. Meier, Nat. Commun. **10**, 1661 (2019).

[25] A. L. Kholkin, S. V. Kalinin, A. Roelofs, and A. Gruverman, *Scanning Probe Microscopy* (Springer, New York, 2007), Vol. 2, pp. 173–214.

[26] S. Prosandeev, D. Wang, W. Ren, J. Íñiguez, and L. Bellaiche, Adv. Funct. Mater. **23**, 234 (2013).

[27] S. Prosandeev, Y. Yang, C. Paillard, and L. Bellaiche, npj Comput. Mater. **4**, 8 (2018).

[28] D. Wang, J. Weerasinghe, and L. Bellaiche, Phys. Rev. Lett. **109**, 067203 (2012).

[29] J. L. García-Palacios and F. J. Lázaro, Phys. Rev. B **58**, 14937 (1998).

[30] See Supplemental Material at http://link.aps.org/supplemental/10.1103/PhysRevMaterials.6.124404 for details on the effect of temperature on the results.

[31] J. Hlinka, M. Paściak, S. Körbel, and P. Marton, Phys. Rev. Lett. **119**, 057604 (2017).

[32] B. Xu, J. Íñiguez, and L. Bellaiche, Nat. Commun. **8**, 15682 (2017).

[33] S. Boyn, J. Grollier, G. Lecerf, B. Xu, N. Locatelli, S. Fusil, S. Girod, C. Carrétéro, K. Garcia, S. Xavier, J. Tomas, L. Bellaiche, M. Bibes, A. Barthélémy, S. Saïghi, and V. Garcia, Nat. Commun. **8**, 14736 (2017).

[34] P. Rovillain, R. De Sousa, Y. Gallais, A. Sacuto, M. Méasson, D. Colson, A. Forget, M. Bibes, A. Barthélémy, and M. Cazayous, Nat. Mater. **9**, 975 (2010).

[35] M. Cazayous, D. Malka, D. Lebeugle, and D. Colson, Appl. Phys. Lett. **91**, 071910 (2007).

[36] R. P. S. M. Lobo, R. L. Moreira, D. Lebeugle, and D. Colson, Phys. Rev. B **76**, 172105 (2007).

[37] R. Haumont, J. Kreisel, P. Bouvier, and F. Hippert, Phys. Rev. B **73**, 132101 (2006).

[38] S. Kamba, D. Nuzhnyy, M. Savinov, J. Šebek, J. Petzelt, J. Prokleška, R. Haumont, and J. Kreisel, Phys. Rev. B **75**, 024403 (2007).